Published in final edited form as:

Build Environ. 2022 January ; 207(Pt A): . doi:10.1016/j.buildenv.2021.108465.

Development and validation of a dynamic mass-balance prediction model for indoor particle concentrations in an office room

Soo Bhin Park[a,1], **Ju-Hyeong Park**[b,1], **Young Min Jo**[c,1], **Doosam Song**[d,1], **Sujeong Heo**[c], **Tae Jeong Lee**[c], **Sowoo Park**[d], **Junemo Koo**[a,*]

[a]Department of Mechanical Engineering, College of Engineering, Kyung Hee University, Yong-In, Gyung-Gi Do, South Korea

[b]National Institute for Occupational Safety and Health, Respiratory Health Division, Morgantown, WV, USA

[c]Department of Environmental Science and Environmental Engineering, College of Engineering, Kyung Hee University, Yong-In, Gyung-Gi Do, South Korea

[d]School of Civil, Architectural Eng., and Landscape Architecture, Sungkyunkwan University, Suwon, 16419, South Korea

Abstract

The Korean government recommends intermittent operation of air purifiers (APs) as a measure to maintain indoor particulate matter (PM) concentrations below the mandatory standards and reduce exposure to indr $PM_{2.5}$ (PM with a diameter smaller than 2.5 μm). However, there is no guideline to inform occupants of when and how long APs should be operated to comply with the standards. In this study, we developed a dynamic mass-balance model to predict indoor PM concentrations in an office considering penetration of outdoor particles, change in number of occupants, and operational status of the AP. The model fit and prediction accuracies were verified using the American Society for Testing and Materials (ASTM) D 5157 criteria and the k-fold validation technique. We observed that indoor $PM_{2.5}$ concentrations were determined by infiltration of outdoor $PM_{2.5}$, and indoor generation/resuspension by occupants and removal. For $PM_{2.5-10}$($2.5\ \mu m < \text{diameter} < 10\ \mu m$), the indoor concentrations were determined by interior door access and indoor generation/resuspension. The operation of an AP effectively decreased indoor $PM_{2.5}$ concentration but not $PM_{2.5-10}$. We found that our model accurately predicted indoor PM concentrations. Therefore, using the developed model, a guideline may recommend: 1) start the AP when the predicted indoor $PM_{2.5}$ concentrations under no AP operation approached the standard (e.g., 90% of the standard); and 2) stop the AP when the indoor $PM_{2.5}$ concentration

*Corresponding author. jmkoo@khu.ac.kr (J. Koo).

[1]These authors contributed equally.

Disclaimer

The findings and conclusions in this report are those of the authors and do not necessarily represent the official position of the National Institute for Occupational Safety and Health, Centers for Disease Control and Prevention.

Declaration of competing interest

The authors declare that they have no known competing financial interests or personal relationships that could have appeared to influence the work reported in this paper.

predicted under the assumption of no AP operation fell below the standard (e.g., 80% of the standard).

Keywords

Particulate matter; I/O ratio; Infiltration factor; Penetration factor; Air purifier; Prediction model

1. Introduction

Exposure to $PM_{2.5}$ (particulate matter with an aerodynamic diameter smaller than $2.5\ \mu m$) has been causally associated with respiratory and cardiovascular diseases [1]. Every year, Korea experiences frequent events of high outdoor concentrations of $PM_{2.5}$ due to urbanization and yellow dust transported from Mongolia and China [2–4]. In Korea, outdoor air quality is managed by the Clean Air Conservation Act (CACA) and the government issues warnings to the public during high outdoor $PM_{2.5}$ concentration events [5]. When the warnings are issued, the government implements control measures to reduce the outdoor concentrations. During the warnings, the government recommends that people stay indoors with windows and doors closed or wear a mask if they need to be outside [6,7]. Consequently, people spend even more time indoors than usual. Therefore, to minimize public exposure to outdoor $PM_{2.5}$ that has infiltrated indoor environments, the Korean government also manages indoor $PM_{2.5}$ concentrations with the Indoor Air Quality Control Act [8] or the School Health Act [9] depending on the type of indoor space.

In 2018, the Korea Ministry of Environment reinforced the ambient $PM_{2.5}$ standard from annual mean concentration of $25\ \mu g/m^3$ (daily mean of $50\ \mu g/m^3$) to $15\ \mu g/m^3 \left(35\ \mu g/m^3\right)$ to further reduce population exposures [10]. Accordingly, the government operates the outdoor PM forecast and public warning system that guides the public to reduce their exposure to outdoor $PM_{2.5}$. According to the air pollution standards of the Korean CACA, the Office of Education has to prepare an air pollution response manual to manage indoor PM concentrations according to the recommendations of the PM forecast and public warning system [7]. As stated by the manual, indoor PM concentrations should be maintained below $35\ \mu g/m^3$ for $PM_{2.5}$ and $75\ \mu g/m^3$ for PM_{10}. Indoor air quality (IAQ) managers should operate air filtration systems intermittently to comply with the standards if the indoor $PM_{2.5}$ concentration is expected to exceed the standard because of the excessive inflow of high concentrations of outdoor PM. However, to comply with the guideline, IAQ managers need to determine: 1) on which days they should operate the air purifiers (APs); and 2) during the day when they should start and stop the APs to comply with the standards. To provide the IAQ managers with an appropriate guideline, first we should understand how AP operation modifies the relationships between indoor and outdoor PM concentrations, and then develop accurate indoor PM prediction models to inform the IAQ managers of when they should operate AP.

To illustrate the relationships between indoor and outdoor PM concentrations, Chen and Zhao [11] summarized experimental and modeling studies and discussed the ratio of indoor to outdoor concentrations (I/O ratio), the infiltration factor, and the penetration factor. They concluded that the mass-balance models using the I/O ratios and the infiltration factors did not sufficiently reflect the impact of the time-varying concentrations of outdoor PMs because the ratios and factors were defined based on the assumption of an equilibrium state that is rarely achieved in real life. And they found that the dynamic models simultaneously considering the effects of variable outdoor PM infiltration, and indoor removal and generation on indoor PM concentrations were best suited for describing time-varying indoor PM concentrations. They reported that the external wind environment was unsteady and irregular, which affected the momentary infiltration of outdoor PMs into indoors. Martin and Graça [12] wrote a review paper on $PM_{2.5}$ sources and sinks in urban indoor and outdoor environments, variation in I/O ratios with building type, prediction of indoor $PM_{2.5}$ level, differences in exposure limits between countries, and indoor $PM_{2.5}$ exposure reduction methods. Choi and Kang [13] evaluated the infiltration factors of PMs in 11 residential homes in South Korea after the indoor and outdoor pressure difference was fixed at 10 Pa that far exceeded the actual range (0–5 Pa) of the measured pressure differential. Their estimated mean infiltration factor was 0.65 with a range of 0.38–0.88.

On the other hand, the use of APs indoors affects the indoor PM concentrations and thus the I/O ratios. Shaughnessy and Sextro [14] defined performance metrics of APs as the clean air delivery rate (CADR) and effectiveness (ε). CADR represents the capability of providing a clean air supply, while the effectiveness is assessed as the benefit of using an AP in the context of its actual use. They showed that the effectiveness was affected by particle deposition rate and, hence, by particle size. Cox et al. [15] demonstrated that portable APs using high efficiency particulate air filtration could effectively remove traffic-related airborne ultrafine particles. Pei et al. [16] analyzed the effects of portable APs on reduction of indoor PM levels and reported that portable APs were widely used in South Korea. They reported that 81.4% of the investigated AP owners did not use APs at all and 18.6% used AP occasionally for 1–4 h a day on the mode with low or medium airflow. The main reasons not constantly using AP were increased energy consumption and noise. Noise also made the users manipulate AP operation, which had a negative impact on indoor PM reduction. Recently, Huang et al. [17] demonstrated that auto-mode air purifier operation, during which the air flow rate was controlled automatically based on the surrounding PM concentrations, was superior to manual operation. The random user manipulation of the AP based on personal preference and not following guidelines would have negative effect on indoor PM reduction. Therefore, a program of operation should be developed to maximize the effectiveness of AP use and save energy.

In analyzing the relationships between indoor and outdoor PM concentrations, application of the machine learning technique is increasingly popular. Wei et al. [18] published a review article summarizing 37 studies on IAQ predictions including $PM_{2.5}$. They reported that the physical model without using the machine learning technique was suitable for cases in which the PM transport mechanism was obvious; however, statistical methods using machine learning were more practical if a large dataset was available although the transport mechanism was not apparent.

In our study, we aimed to develop useful guidance that can assist IAQ managers to develop a protocol for an AP operation schedule to maintain indoor PM concentrations below the standard levels. To this end, 1) three-week-monitoring data of indoor and outdoor PM concentrations in an office at a university were analyzed to identify the transport mechanism; 2) a governing differential equation for indoor PM concentrations was derived to explain the mechanism; and 3) a model to predict indoor PM concentrations was developed by solving the differential equation using a machine learning technique with the input of the forecasted outdoor PM concentration data.

2. Theory and experimental set-up

2.1. Details of the test area

A schematic diagram of the tested office space is shown in Fig. 1. The office room, located in the College of Engineering at Kyung Hee University, had an area of 45 m^2 and a ceiling height of 2.5 m, with one exterior window and one interior door from/to the hallway. A portable AP designed for a 60 m^2 room (Model Blue Sky, Samsung, Seoul, South Korea) was installed to abate the indoor PM concentrations. The air purifier was equipped with a pre-filter, an activated carbon filter, and a HEPA filter with filtration efficiency of 99.9% for particles larger than $0.3\ \mu$m. The experiment was conducted in uninterrupted conditions to avoid affecting the occupants' normal behavior. To analyze the impacts of the AP on indoor PM concentrations, experiments were first performed under the condition with no AP operation between December 30, 2020, and January 10, 2021, and then with continuous AP operation between January 11 and January 20, 2021. The number of occupants, the status of the exterior window and interior door opening, and the AP operation over time were recorded in a Microsoft® Excel spreadsheet during the measurement period. The office room was equipped with two fan coil units that only recirculated indoor air without outdoor air intake.

We simultaneously measured PM concentrations outdoors and in the hallway using air quality monitors (IAQ Station-CL1, Kweather, South Korea) at the outdoor and hallway in April 2021 (Fig. 2). According to the manufacturer, the uncertainty of particle sensors using laser light scattering technique in the monitor was ±15% for $PM_{2.5}$ and ±20% for PM_{10}. The hallway $PM_{2.5}$ and PM_{10} concentrations closely followed the pattern of outdoor PM concentrations and the difference was within the uncertainty range. Therefore, for simplicity of model development, we assumed that the concentrations outdoors and in the hallway were the same.

2.2. Mass balance model

The mass balance model equation used in this study is shown in Eq. (1). The model accounted for PM intrusion from outdoors caused by increases in air change rate from occupants' door access and particles generated per person with the number of occupants.

$$\frac{dC_{in}}{dt} = ACH \cdot (P + PO \cdot |\Delta R|) \cdot C_{out}(t) - (ACH + k_d + k_{AP}) \cdot C_{in}(t) + \dot{s} \cdot R \tag{1}$$

where C_{in}: indoor PM concentration (# /m^3, μg/m^3),

C_{out}: outdoor PM concentration ($\# / \mathrm{m}^3, \mu \mathrm{g/m}^3$),

ACH: air change rate (1/hour),

P: effective penetration factor (no unit) accounting for particle intrusions from outside the office room through all cracks in the walls when all doors and windows are closed,

PO: coefficient {1/(hour × door access)} for additional PM penetration induced by the occupants' entering or exiting the room by opening and closing the door,

ΔR: number of occupants' door accesses for a given time interval. The absolute value was used to consider the increased air exchange by door access even with a decrease in number of occupants.

k_d: particle deposition rate (1/hour),

k_{AP}: particle removal rate using air purifier (1/hour),

$\dot{s}$: particle generation or resuspension rate per person (# or $\mu \mathrm{g/m3/person/hour}$),

R: number of occupants in the room.

To determine the coefficients for Eq. (1), the indoor and outdoor PM concentrations were collected using optical particle counters with 31 channels in particle size (between 0.25 and $32\ \mu\mathrm{m}$) (Model 11-A GRIMM Aerosol Technik, Ainring, Germany). Of the 31 channels, only 23 channels collecting up to $10\ \mu\mathrm{m}$ were analyzed for the study. The number concentration was measured and then converted to the mass concentration, and the aggregated concentrations for $PM_{2.5}$ and PM_{10} were also calculated. We considered penetration coefficient (P) and deposition rate (k) modified by the air exchange rate (ACH) ($P' = ACH \cdot P$; $PO' = ACH \cdot PO$; and $k' = ACH + k_d + k_{AP}$) in the model because the amount of infiltration and deposition varied by outdoor wind speed/direction and occupant's door access [11].

2.3. Application of machine learning technique

Conventional machine learning produces a black-box model derived by using sampled data without accounting for system structure; however, Ma [19] defined a grey model to have a deterministic structure with model parameters that are estimated by sampled data. In this study, Equation (1) was used as the dynamic structure in the form of a differential equation to explain dynamic relation between outdoor and indoor concentrations where the four model parameters (P', PO', k', and s) were estimated. Developing predictive models using machine learning generally requires sequential steps including determining model parameters and evaluating model fitting and predictive accuracy.

The measured indoor and outdoor PM concentrations, the first derivative of indoor PM concentration with respect to time, and the history of occupancy were plugged into Eq. (1). Then, the four model coefficients (P', PO', k', and $\dot{s}$) were determined using the least-squares method to minimize the deviation between left-hand and right-hand terms of Eq. (1). The open source statistical environment, R and DEop-tim [20] and minpack.lm [21] packages were used for all calculations [22].

The fitting and prediction accuracies of the developed model were validated according to the American Society for Testing and Materials (ASTM) D 5157 that provided the standard guide for statistical evaluation of the IAQ model [23]. In this study, the model performance metrics were the correlation coefficient (r), slope (b), and intercept (a) of the linear regression between the observed and model-predicted values, normalized mean squared error (NMSE), fractional bias (FB), and similar index of bias based on variance (FS). They were calculated as shown in Eqs. (2)–(7):

$$r = \frac{\sum_{i=1}^{n}\left[\left(C_{oi} - \overline{C}_o\right)\left(C_{pi} - \overline{C}_p\right)\right]}{\sqrt{\left[\sum_{i=1}^{n}\left(C_{oi} - \overline{C}_o\right)^2\right]\left[\sum_{i=1}^{n}\left(C_{pi} - \overline{C}_p\right)^2\right]}} \tag{2}$$

$$b = \frac{\sum_{i=1}^{n}\left[\left(C_{oi} - \overline{C}_o\right)\left(C_{pi} - \overline{C}_p\right)\right]}{\sqrt{\left[\sum_{i=1}^{n}\left(C_{oi} - \overline{C}_o\right)^2\right]}} \tag{3}$$

$$a = \overline{C}_p - b\overline{C}_o \tag{4}$$

$$NMSE = \frac{\overline{\left(C_p - C_o\right)^2}}{\overline{C}_o \cdot \overline{C}_p} \tag{5}$$

$$FB = 2 \cdot \frac{\left(\overline{C}_p - \overline{C}_o\right)}{\left(\overline{C}_p + \overline{C}_o\right)} \tag{6}$$

$$FS = 2 \cdot \frac{\left(\sigma_{C_p}^2 - \sigma_{C_o}^2\right)}{\left(\sigma_{C_p}^2 + \sigma_{C_o}^2\right)} \tag{7}$$

where C_o, C_p, i, and σ^2 represent the observed data, model predictions, index, and variance, respectively. A bar over a symbol represents the mean value. The acceptable ranges of the model performance metrics for an adequate model were $r \geq 0.9,\ 0.75 \leq b \leq 1.25,\ |a| \leq 0.25\overline{C}_o,\ NMSE \leq 0.25,\ |FB| \leq 0.25$, and $|FS| \leq 0.5$.

The fitting accuracy is the measure of how closely the model-fitted values represent the actual measurements. In contrast, the prediction accuracy describes how accurately the developed model predicts actual PM measurements in test data or unmeasured concentrations. In machine learning, the k-fold validation was used to assess the prediction accuracy of the developed models. This method divides all of the data into k datasets, develops a model using k-1 datasets, and uses the remaining dataset as a test dataset [24]. In our study, all measured data were grouped into 21 datasets by the day of the measurement. Then a model was developed with the combined data of 20 datasets, and the remaining test data were used to compare with the PM concentrations predicted by the developed model. This process was repeated 20 times with various test data. The accuracy of the predicted data was evaluated with the k-fold validation test using the six performance metrics above.

The effectiveness of AP (ε) was also evaluated. And it was defined as follows:

$$\varepsilon = \frac{C_{in}^{AP\,OFF} - C_{in}^{AP\,ON}}{C_{in}^{AP\,OFF}} \tag{8}$$

where $C_{in}^{AP\,OFF}$ and $C_{in}^{AP\,ON}$ represent the measured or predicted indoor PM concentrations when the AP is off or on, respectively.

3. Results and discussion

3.1. Analysis of raw data

Fig. 3 (a)–(d) compare the number concentrations of indoor and outdoor PMs by particle size. Of the 23 channels shown in Table 1, four channels (0.265, 0.900, 2.250, and 9.250 μm) were selected to show the overall trend of changes in concentrations over time. The indoor PM concentrations measured from the smallest channel (0.265 μm) were similar to and followed the pattern of changes in outdoor PM concentrations while the AP was not being operated (unshaded area in Fig. 3). As particle size increased, the indoor PM concentrations were lower than the outdoor PM concentrations but continued to follow the pattern of changes in outdoor PM. In the largest particle size channel (9.250 μm), particles were not detected in the indoor air most of the time. During AP operation (shaded area in yellow in Fig. 3), the indoor PM concentrations from the smallest particle channel (0.265 μm) were much lower than outdoors and the difference was evident compared to other channels. Generally, the indoor concentrations from all channels were lower during the period of AP operation than no AP operation although the outdoor PM concentrations were higher during the period of AP operation than no AP operation.

Fig. 4 shows the average values of the ratios of indoor to outdoor PM number concentrations over the measurement time in all channels by AP operation. When the AP was not running, the ratio was close to 1 for the smallest particle channel but decreased as particle size increased. On the other hand, when the AP was in operation, the ratio decreased in all channels, with greater reduction for smaller particles ($\leq 3.0\ \mu$m in diameter) than larger particles ($> 3.0\ \mu$m). The analyses using mass concentration data showed a similar pattern to those using the number concentrations. These differential effects by particle size can be explained by the mass balance of the effects of the three factors (particle penetration, particle removal, and generation mechanism by particle size). The indoor transmission mechanism of external particles determined with Eq. (1) will be discussed in detail in a later section.

3.2. Model development

The indoor PM concentrations with AP in operation shown in Fig. 3 are the result of the mass balance of particle penetration, settling by gravity on indoor surfaces, surface adsorption, particle removal by AP, and particle generation by occupants. By plugging the measured indoor and outdoor PM concentrations and the number of occupants into Eq. (1), the model coefficients were calculated using the least-squares method. When we developed the model, we assumed that AP operation only affected particle removal but not particle penetration and generation. In other words, among the model coefficients obtained using the data measured without AP operation, P', PO', and $\dot{s}$ stayed the same regardless of AP operation, while k' changes by the k_{AP} term in Eq. (1) that is activated by AP operation.

The model coefficients determined by particle size using PM number concentration data are shown in Fig. 5. The coefficient P', representing the modified (by ACH) penetration of external PM into indoors, peaked in the $0.265\ \mu$m and $2.25\ \mu$m size channels, indicating that penetration of PM from outdoors was the largest ($P' > 0.05$) at the particle sizes smaller than $0.45\ \mu$m and between 1 and $3\ \mu$m. Considering that the ACH was constant regardless of particle size (Fig. 5(a)), the shape and changing pattern of penetration factor P by particle size would be the same as those of P'. The value of P' was low at particle sizes between 0.45 and $1\ \mu$m and approached zero for dust particles larger than $3\ \mu$m in diameter, indicating that particles in those ranges in size do not effectively penetrate the building envelope. The model constant k' (particle deposition or removal rate) gradually increased with particle size in the period of no AP operation (Fig. 5(b)), indicating an increase in gravitational settling with increasing mass of larger particles. When the AP was in operation, the model constant k' substantially increased for all PM sizes compared to that for no AP operation since the AP filtered indoor particles. The deposition rate peaked at approximately $3\ \mu$m-size particles and then became unstable because the measured indoor PM number concentrations were extremely low (<10), and the detection by the particle counter became discontinuous (Fig. 3(d) in the previous section). The determined PO', representing the effect of additional penetration by occupant door access, is shown in Fig. 5(c). It started to increase above 0.05 for particles larger than $1.5\ \mu$m in diameter. Fig. 5 (d) also shows that the indoor generation per person ($\dot{s}$) gradually decreased with particle size when the PM number concentration data were used; however, the contributions of larger particles to the PM mass concentration were much more significant than smaller ones when the mass concentration data were used because of high mass of the larger PM. The model parameters using the number concentrations had similar shape and pattern to those using mass concentrations, except for the particle generation coefficient.

The experiments and measurements were performed under normal circumstances without interference, and the effects of particle penetration, removal, and generation were considered simultaneously in the same model. Therefore, the increase in concentrations of indoor PM is a collective effect of particle penetration, occupant door access, and indoor generation and resuspension, and the individual effects could not be separately estimated.

Analysis of PM concentrations from all 23 channels was useful to understand the infiltration mechanisms by particle size. However, we developed a forecast model for the aggregated indoor $PM_{2.5}$ and PM_{10} concentrations because 1) government-forecasted outdoor PM data as the input for the model were available only for $PM_{2.5}$ and PM_{10}; and 2) indoor PM levels in Korea were managed according to the standards for indoor $PM_{2.5}$ and PM_{10} [7]. Fig. 6 compares the measured and model-fitted indoor PM concentrations. The solid lines in the figure represent the measured indoor PM concentrations, and the dashed lines the fitted ones. Although the fitted values generally agreed well with the actual measurements, in some cases the fitted PM_{10} did not meet the inequality condition of $PM_{2.5} \leq PM_{10}$ concentration. To comply with the inequality condition, the model using the $PM_{2.5-10}$ (coarse particles between 2.5 and 10 μm in aerodynamic diameter) data was developed and then coarse particle concentrations were separately fitted. The black dash-dotted line in Fig. 6 represents the fitted values estimated from summing the fitted values for $PM_{2.5}$ and $PM_{2.5-10}$, which always satisfied the inequality condition and improved the model fitting accuracy compared to the fitted values using PM_{10} for modeling.

Table 2 presents the model coefficients determined for $PM_{2.5}$ and coarse particles. The results indicate that the penetration effect was more evident for $PM_{2.5}$ than coarse particles, while the effects of particle removal, occupant door access, and particle generation/ resuspension were larger for coarse particles than for $PM_{2.5}$.

3.3. Model validation

Fig. 7 shows the model performance metrics (r, b, $a/\bar{C}_o$, $NMSE$, FB, and FS) estimated using the actual measurements (C_o) and model fitted values (C_p). The four metrics b, $a/\bar{C}_o$, $NMSE$, and FB met the requirements for an adequate model suggested in ASTM D 5157 for all size channels. The correlation coefficient, r, and the similar index, FS, did not meet the requirements for the channels with larger particle size ≥ 3 μm and ≥ 4 μm, respectively. However, when we used models for $PM_{2.5}$ and PM_{10}, all the model performance metrics satisfied the criteria for an adequate model (Table 3). The prediction accuracies were tested by evaluating the metrics using the k-fold validation method as presented in Table 4. Although the correlation coefficients were marginal, all other metrics met the adequate model requirements. Therefore, the developed predictive model based on indoor and outdoor PM monitoring data, the number of occupants, and the status of AP operation indoors appeared to adequately forecast indoor PM concentrations in an office room.

3.4. Impact analysis of each term in the governing equation

Fig. 8 shows the relative impacts of each term on the right-hand side in the Eq. (1) determining the indoor PM concentrations. The sum of the impacts of all terms was set to 100% in each condition in the figure-i.e., relative impact. For the condition with no occupant and no AP operation (Fig. 8(a)), particle deposition was slightly larger than particle penetration for most particle sizes, which resulted in decreases in the indoor PM concentrations over time. The average indoor PM concentrations for particles larger than $3\ \mu m$ in diameter were lower than $1\ \mu g/m^3$. The concentrations of particles larger than $7\ \mu m$ in diameter decreased below $0.1\ \mu g/m^3$ or to the undetectable level for most of the time.

The particle removal effect was nearly zero in some time periods when the airborne PM concentrations were close to zero. This resulted in an artifact of the highest relative penetration effect, especially for the $9.250\ \mu m$ channel for which the indoor PM concentrations were zero most of the time.

Under the condition with occupants but no AP operation (Fig. 8(b)), the particle removal effect was less than 50% for all particle sizes. The impact of occupant door access on indoor $PM_{2.5}$ concentrations was negligible. The combined effects of particle penetration, indoor particle generation, and resuspension were similar to the effects of particle removal in all channels. In contrast, the particle penetration effects became negligible for coarse particles, and the combined effects of door access and indoor generation/resuspension offset the removal effects. Previous studies [23] have reported similar findings that fine particles infiltrate from the outdoors better than coarse particles, whereas occupant activities mainly contribute to the coarse particles in the indoor air.

The relative effects of AP operation on each term were analyzed (Fig. 8(c) and (d)). As shown in Fig. 5(b) in the earlier section, the coefficient (k') itself under AP operation substantially increased especially in particles larger than $2\ \mu m$ in diameter, compared to that with no AP; however, relative impact of particle removal (deposition) with AP operation on indoor PM concentrations was only moderately increased (Fig. 8(c) and (d)) because the net removal effect is determined by the product term of the deposition coefficient (k') and indoor PM concentrations that significantly decreased during AP operation. Furthermore, the outdoor PM concentrations during the period of AP operation were higher than those during the period of no AP operation, which resulted in increased penetration. The measurable increase in the relative effects of occupant door access on indoor coarse PM concentrations was observed, which was mainly influenced by the combination of high outdoor and low indoor concentrations during the period of AP operation.

3.5. Analysis of air purifier performance

Fig. 9 compares the average indoor and outdoor PM concentrations by particle size and AP operation. The outdoor PM concentrations during the period of AP operation were higher than those during no AP operating as described earlier. Regardless of AP operation, average indoor PM concentrations were lower than outdoor concentrations for all particle sizes. However, the ratio of indoor to outdoor PM concentrations decreased with AP operation compared to without AP operation.

The effectiveness of air purification could be calculated by predicting the indoor PM concentrations using the prediction model, assuming that the AP was operating for the period of no AP operation or vice versa. Fig. 10 shows the measured indoor and outdoor and predicted indoor PM concentrations by AP operation for the smallest particle channel

(0.250 – 0.280 μm), the 2.250 μm channel (2.0 – 2.5 μm), and the integrated $PM_{2.5}$ and PM_{10}. Before January 11, 2021 when the AP was turned on, the predicted concentrations were based on the assumption of AP operation; however, on January 11, 2021 and onward, the predicted concentrations were based on the assumption of no AP operation. The figure indicated that the measured and predicted values were in reasonable agreement in both periods before and after the AP was turned on. Therefore, the developed prediction model appeared to be useful to predict indoor PM concentrations with time-varying outdoor PM concentrations for office rooms with a similar condition.

Fig. 10 (c) and (d) also show the concentrations of measured and predicted $PM_{2.5}$ and PM_{10}, respectively. These two plots demonstrate that the developed model accurately predicted the trends of the time-varying indoor PM concentrations. Therefore, our findings indicate that our dynamic mass-balance model could be used to predict indoor PM concentrations and determine when the AP should be turned on or off to reduce indoor exposure to PM. The Korean government standards for indoor $PM_{2.5}$ and PM_{10} indicate that these concentrations shall not exceed the standards under any condition. To comply with these standards, it could be advised that the AP should be turned on when the predicted indoor PM concentration without AP operation reaches 90% of the standard. On the other hand, when the predicted concentration with an assumption of no AP operation during the period of AP operation is lower than 80% of the standard, it could be advised to turn off the AP.

The shaded areas in Fig. 10 represent the numerator of Eq. (8), i.e., the amount of particle mass concentration removed by AP operation. Fig. 11 presents the variation in estimated effectiveness of the AP used in our study by particle size. The effectiveness was greater than 75% for PM smaller than 1 μm in diameter and significantly decreased as particle size approached the 1 – 3 μm range. Then, it substantially increased for particles approximately 3 – 4 μm in size. For PM larger than 4 μm, again the effectiveness sharply declined. The particle removal effectiveness of the AP for $PM_{2.5}$ and PM_{10} was estimated to be 86.4% and 86%, respectively. The particle removal effectiveness of AP is a complicated function of particle penetration from outdoors, gravitational deposition, flow field in the room, clean air delivery rate (CADR) of the air purifier, and filter characteristics. However, Shaughnessy and Sextro [14] simplified the particle removal effectiveness (ε) as below:

$$\varepsilon = \frac{CADR}{V \cdot k'_{AP\,\mathrm{OFF}} + CADR} \tag{9}$$

where V represents the volume of the office room. Therefore, removal effectiveness would decrease with particle size as shown in Fig. 11 since $k'_{AP\ OFF}$ increases with particle size as shown in Fig. 5(b).

3.6. Prediction model

Fig. 12 shows the data flow of a prediction system for the indoor PM concentrations developed in this study. First, data of the indoor and outdoor PM concentrations, occupant history, and AP operation history are collected for three or more weeks. The indoor PM concentration prediction model could be developed using Eq. (1) as described in the previous sections. Then the time-varying indoor PM concentrations could be predicted using the developed model with the new input data of the outdoor PM forecast data, expected occupancy, and AP operation schedule. The AP operation schedule to control the indoor PM concentrations can be developed based on the predicted indoor concentrations as shown by the solid arrows in Fig. 12. The accuracy of the prediction model (dash-dotted arrows) could be further evaluated if the monitoring data of indoor PM were available. Then the initial prediction model might be improved by either calculating new model coefficients or reformulating the governing equation.

The Korean government has implemented a PM sensor rating system since 2019. The products with the best performance should meet 80%, 80%, and 0.8 or higher values for the repeatability, accuracy, and determination coefficient, respectively. We are planning to develop an intelligent strategy to help occupants develop a schedule for indoor $PM_{2.5}$ abatement using our study findings to develop a prediction model and indoor monitoring data using low-cost sensor technology, instead of relying on data from expensive and noisy particle counters. Indoor PM measurement data, if available, would help to develop improved prediction models to provide accurate recommendations on AP operation to reduce indoor PM exposure in occupants.

It was challenging to consider particle size composition when estimating the effective penetration factor (P') using the integrated PM concentrations. For example, more outdoor PM would penetrate indoors if smaller particles are dominant in the size distribution of the outdoor PM. Since the size distributions of PM are different in every environment, prediction errors can occur and thus a correction method is needed. As shown in the previous section, the use of $PM_{2.5}$ and $PM_{2.5-10}$ instead of PM_{10} in modeling might alleviate this problem since it allows the model to partly reflect the size distribution of PM.

4. Conclusions

The motivation for this study was to answer the question of when to start and stop indoor air purifiers to comply with the government’s practical guidelines and thus reduce indoor exposures from infiltrated outdoor $PM_{2.5}$ during high outdoor PM concentration events. Using the data of indoor and outdoor $PM_{2.5}$ concentrations, occupancy, and door access histories, we developed a dynamic mass-balance model with which future indoor PM concentrations could be accurately predicted. The model accounted for the time-varying particle penetration from outdoors, indoor particle removal, effects of occupant door access, and internal particle generation/resuspension to predict the dynamic indoor PM concentrations. From our study, we found that the developed model could be used to predict the indoor PM concentrations for $PM_{2.5}$ and PM_{10}. Our model can be used to inform IAQ managers or occupants of when to turn on or off the AP to maintain indoor PM levels below the standards. This information could also maximize effectiveness of AP use and save energy through optimization of operational costs. If indoor monitoring data are available, model prediction could be improved through validating and adjusting the estimated model coefficients.

Acknowledgments

This study was supported by a grant from the National Research Foundation of Korea (NRF) (2019M3E7A1113079) funded by the Korean government (MSIT, MOE).

References

[1]. Englert N, Fine particles and human health - a review of epidemiological studies, in: Toxicol. Lett, Elsevier, 2004, pp. 235–242, 10.1016/j.toxlet.2003.12.035

[2]. gon Ryou H, Heo J, Kim SY, Source apportionment of PM10 and PM2.5 air pollution, and possible impacts of study characteristics in South Korea, Environ. Pollut 240 (2018) 963–972, 10.1016/j.envpol.2018.03.066. [PubMed: 29910064]

[3]. Choi J, Park RJ, Lee HM, Lee S, Jo DS, Jeong JI, Henze DK, Woo JH, Ban SJ, Do Lee M, Lim CS, Park MK, Shin HJ, Cho S, Peterson D, Song CK, Impacts of local vs. trans-boundary emissions from different sectors on PM2.5 exposure in South Korea during the KORUS-AQ campaign, Atmos. Environ 203 (2019) 196–205, 10.1016/j.atmosenv.2019.02.008.

[4]. Oh HR, Ho CH, Koo YS, Baek KG, Yun HY, Hur SK, Choi DR, Jhun JG, Shim JS, Impact of Chinese air pollutants on a record-breaking PMs episode in the Republic of Korea for 11–15 January 2019, Atmos. Environ 223 (2020), 117262, 10.1016/j.atmosenv.2020.117262.

[5]. CLEAN AIR CONSERVATION ACT, 16266, 2019. https://elaw.klri.re.kr/kor_mobile/viewer.do?hseq=49746&type=sogan&key=16. (Accessed 21 May 2021).

[6]. Lin Y, Zou J, Yang W, Li C-Q, A review of recent advances in Research on PM2.5 in China, Int. J. Environ. Res. Publ. Health 15 (2018) 438, 10.3390/ijerph15030438.

[7]. Seoul Metropolitan Office of Education, Practical Manual for Dealing with High Concentration of Fine Dust, 2019. http://buseo.sen.go.kr/view/jsp/bbsDownload.jsp?bbsCd=94&bbsSeq=328&orderNo=1.

[8]. INDOOR AIR QUALITY CONTROL ACT, 15583, 2018. https://elaw.klri.re.kr/kor_mobile/viewer.do?hseq=48555&type=sogan&key=16. (Accessed 21 May 2021).

[9]. SCHOOL HEALTH ACT, 16339, 2019. https://elaw.klri.re.kr/kor_mobile/viewer.do?hseq=50148&type=sogan&key=2. (Accessed 21 May 2021).

[10]. (in Korean), News from the Ministry of Environment - Reinforcement of PM2.5 Level to the Those of USA and Japan, 2018, http://www.me.go.kr/home/web/board/read.do?menuId=286&boardMasterId=1&boardCategoryId=39&boardId=849570. (Accessed 25 May 2021).

[11]. Chen C, Zhao B, Review of relationship between indoor and outdoor particles: I/O ratio, infiltration factor and penetration factor, Atmos. Environ 45 (2011) 275–288, 10.1016/j.atmosenv.2010.09.048.

[12]. Martins NR, Carrilho da Graça G, Impact of PM2.5 in indoor urban environments: a review, Sustain. Cities Soc 42 (2018) 259–275, 10.1016/j.scs.2018.07.011.

[13]. Choi DH, Kang DH, Infiltration of ambient PM2.5 through building envelope in apartment housing units in Korea, Aerosol Air Qual. Res 17 (2017) 598–607, 10.4209/aaqr.2016.06.0287.

[14]. Shaughnessy RJ, Sextro RG, What is an effective portable Air cleaning device? A Review, 3, 2007, pp. 169–181, 10.1080/15459620600580129.

[15]. Cox J, Isiugo K, Ryan P, Grinshpun SA, Yermakov M, Desmond C, Jandarov R, Vesper S, Ross J, Chillrud S, Dannemiller K, Reponen T, Effectiveness of a portable air cleaner in removing aerosol particles in homes close to highways, Indoor Air 28 (2018) 818–827, 10.1111/INA.12502. [PubMed: 30133950]

[16]. Pei J, Dong C, Liu J, Operating behavior and corresponding performance of portable air cleaners in residential buildings, China, Build. Environ 147 (2019) 473–481, 10.1016/j.buildenv.2018.08.009.

[17]. Huang CH, Xiang J, Austin E, Shirai J, Liu Y, Simpson C, Karr CJ, Fyfe-Johnson AL, Kronborg Larsen T, Seto E, Impacts of using auto-mode portable air cleaner on indoor PM2.5 levels: an intervention study, Build. Environ 188 (2021), 107444, 10.1016/J.BUILDENV.2020.107444.

[18]. Wei W, Ramalho O, Malingre L, Sivanantham S, Little JC, Mandin C, Machine learning and statistical models for predicting indoor air quality, Indoor Air 29 (2019) 704–726, 10.1111/ina.12580. [PubMed: 31220370]

[19]. Ma X, A brief introduction to the grey machine learning, J. Grey Syst 31 (2018) 1–12. https://arxiv.org/abs/1805.01745v2. (Accessed 7 October 2021).

[20]. Ardia D, Mullen KM, Peterson BG, Ulrich J, {DEoptim}: Differential Evolution in {R}, 2020. https://cran.r-project.org/package=DEoptim.

[21]. Elzhov TV, Mullen KM, Spiess A-N, Bolker B, minpack.lm: R Interface to the Levenberg-Marquardt Nonlinear Least-Squares Algorithm Found in MINPACK, Plus Support for Bounds, 2016. https://cran.r-project.org/package=minpack.lm.

[22]. R Core Team, R: A Language and Environment for Statistical Computing, 2019. https://www.r-project.org/.

[23]. Conshohocken W, Standard Guide for Statistical Evaluation of Indoor Air Quality Models, 1, 2013, pp. 3–6, 97.

[24]. Kuhn M, Johnson K, Applied Predictive Modeling with Applications in R, 2013. http://appliedpredictivemodeling.com/s/Applied_Predictive_Modeling_in_R.pdf.

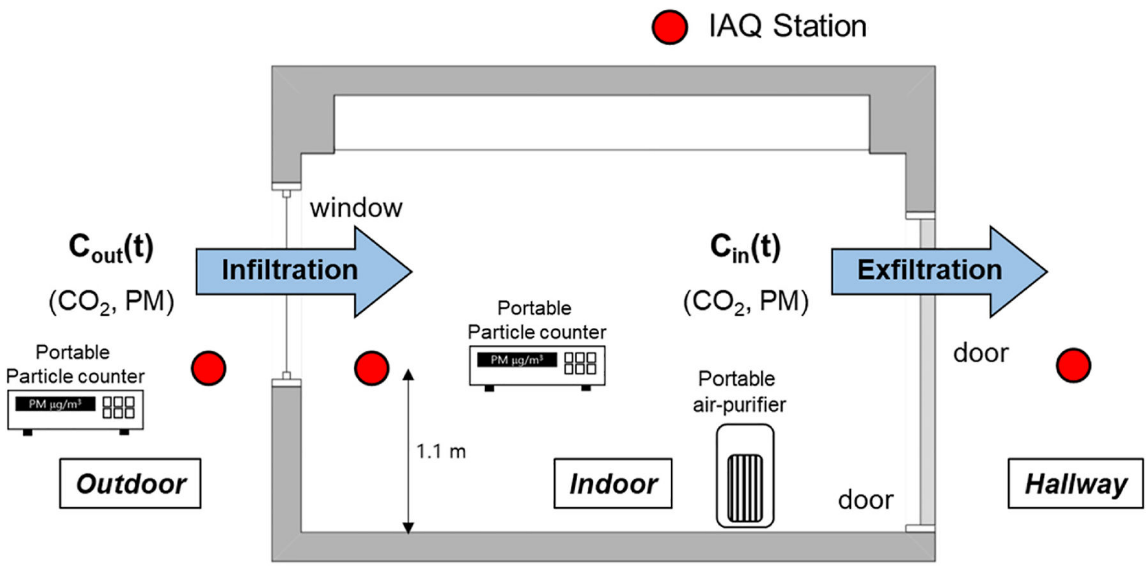

Fig. 1.

Schematic diagram of the experimental office area and instrument setup. $C_{in}(t)$: indoor PM concentration at time t; $C_{out}(t)$: outdoor PM concentration at time t; PM: particulate matter; CO_2: carbon dioxide.

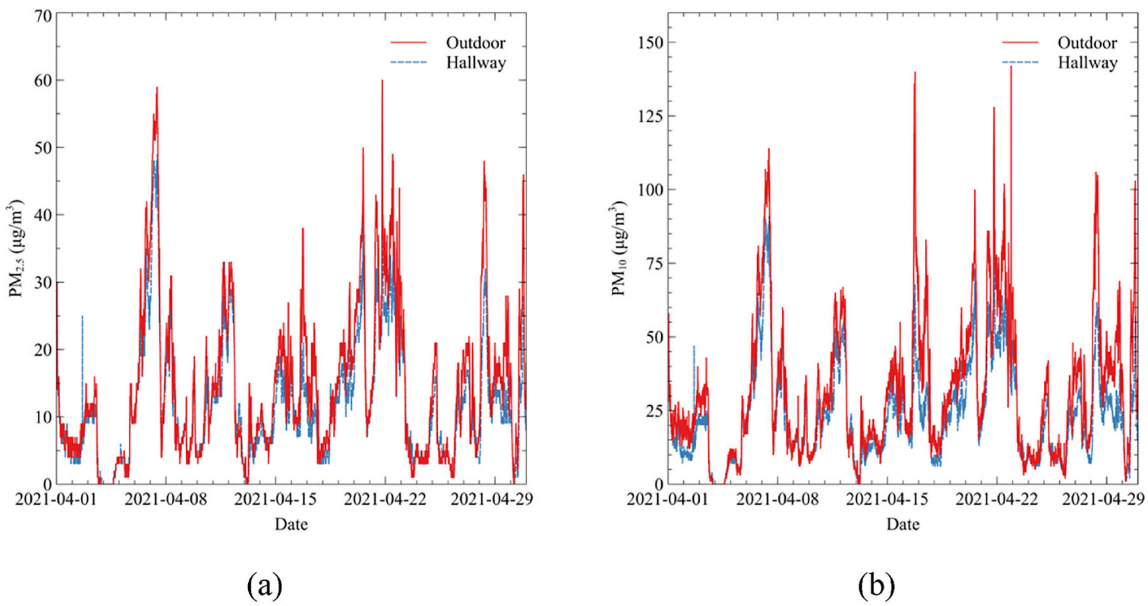

Fig. 2.

Comparison of (a) PM2.5 and (b) PM10 concentration measurements.

Author Manuscript
Author Manuscript
Author Manuscript

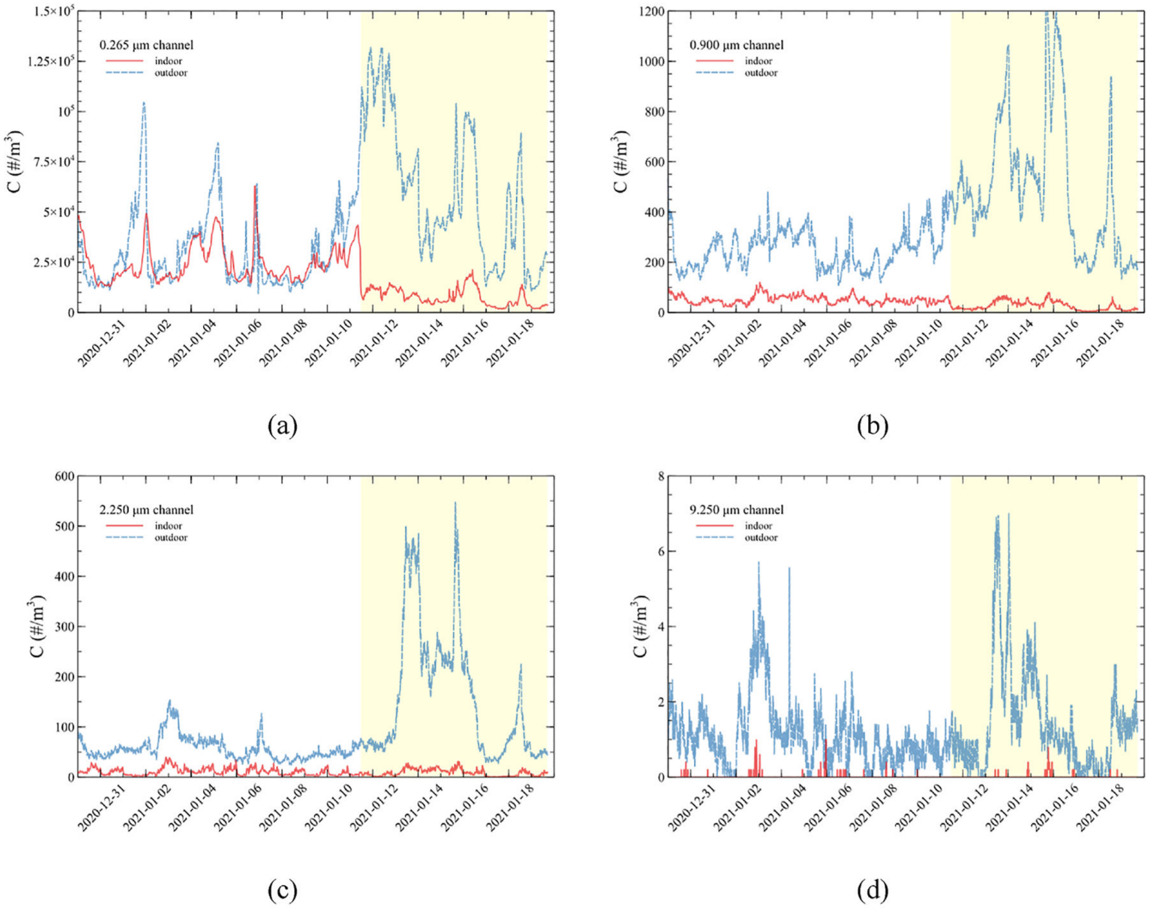

Fig. 3.

Indoor and outdoor particle number concentrations from the four selected channels (0.265, 0.900, 2.250, and 9.250 μm). The shaded areas represent the period when the air purifier was in operation.

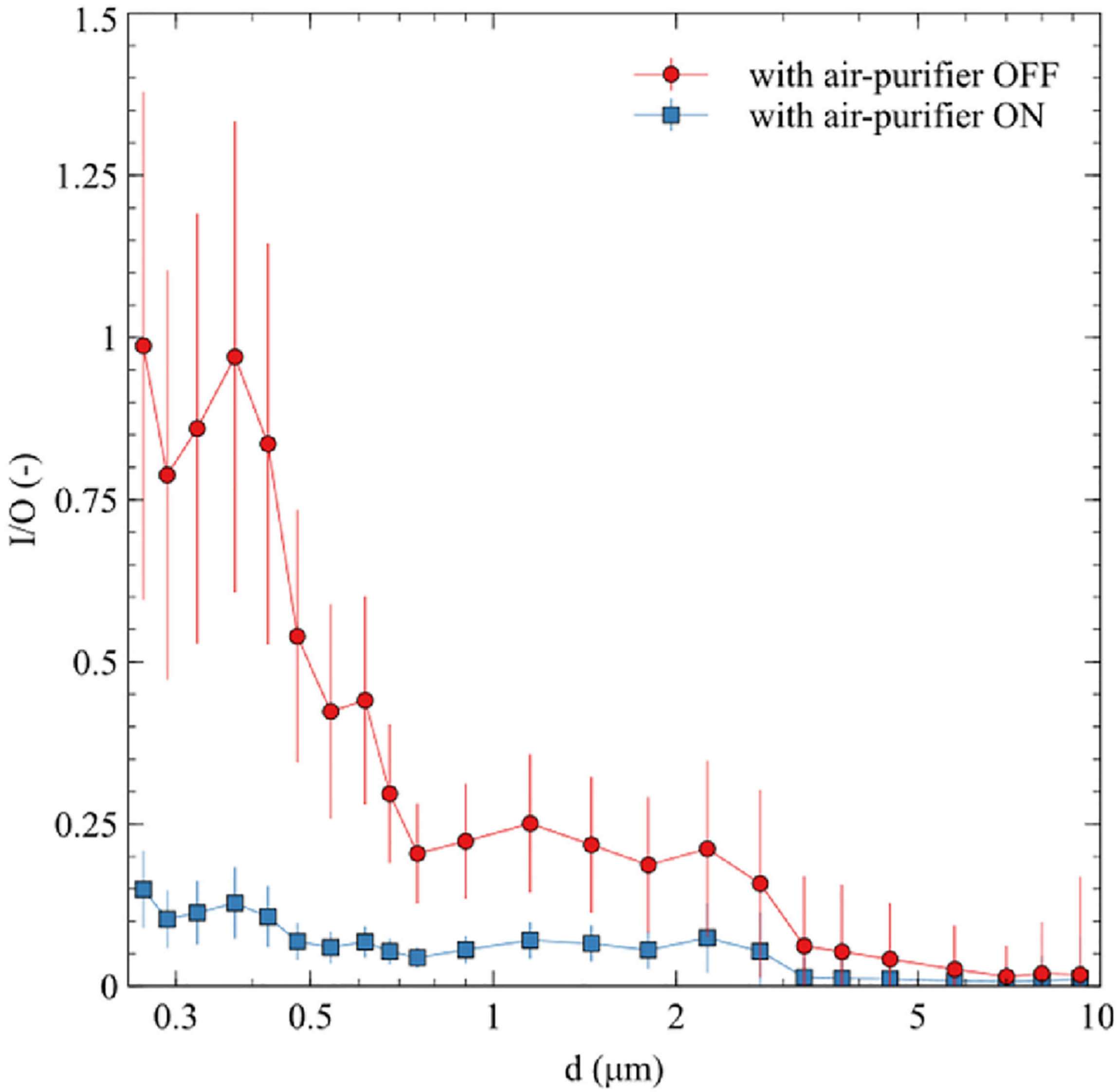

Fig. 4.

Average values of the ratios of indoor to outdoor particle concentrations over the measurement time period by AP operation. The error bars represent one standard deviation of the ratios.

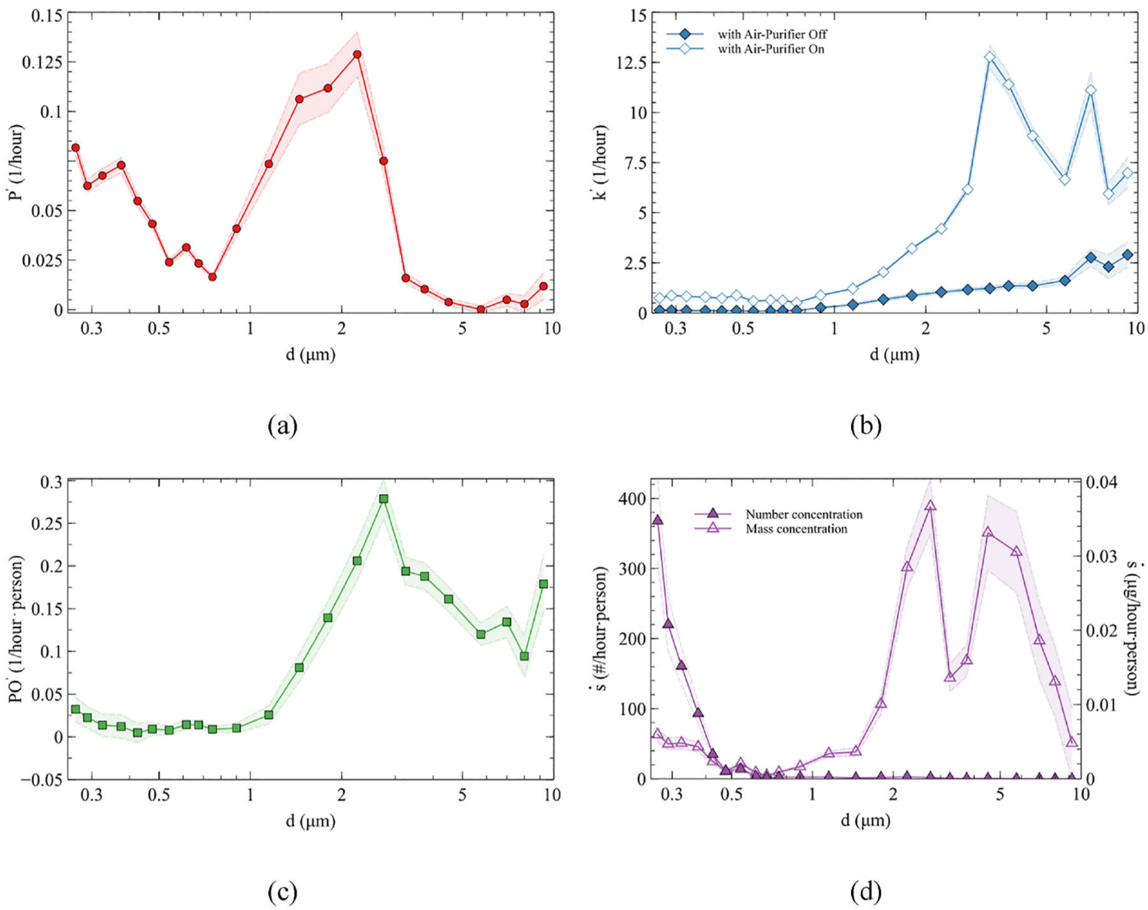

Fig. 5.
Model parameters estimated using Eq. (1): (a) P', (b) k', (c) PO', and (d) $\dot{s}$, where the shaded areas represent the 95% confidence interval.

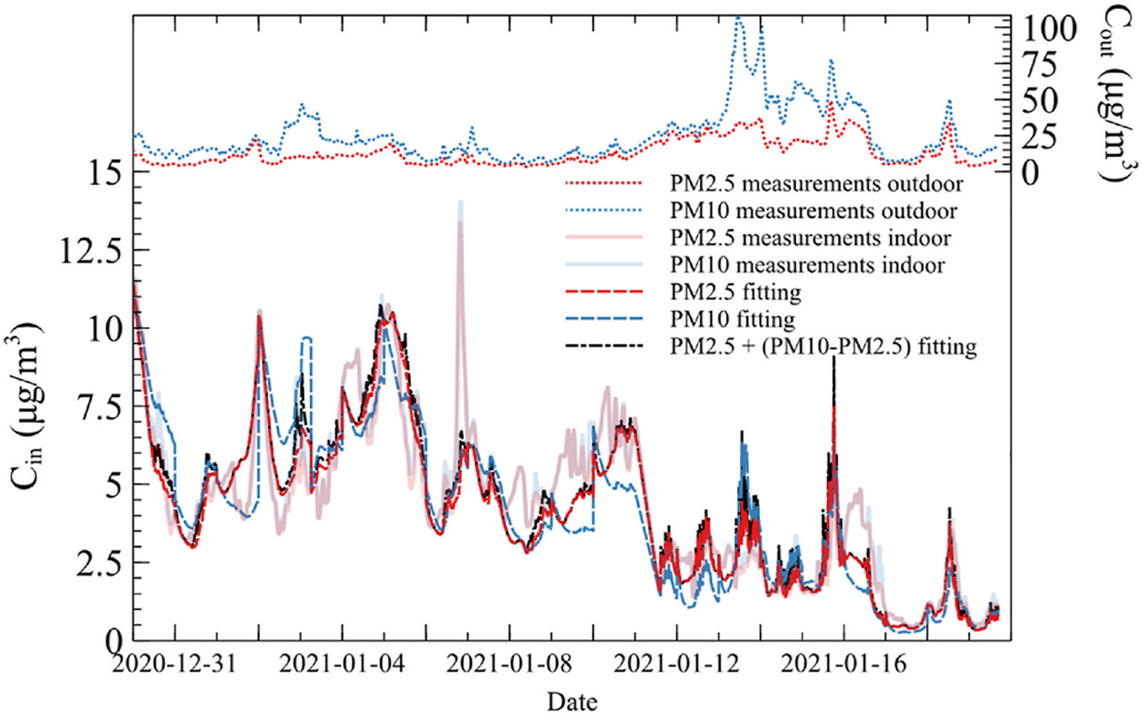

Fig. 6.

Comparison of the model-fitted values with actual measurements of indoor and outdoor $PM_{2.5}$ and PM_{10}.

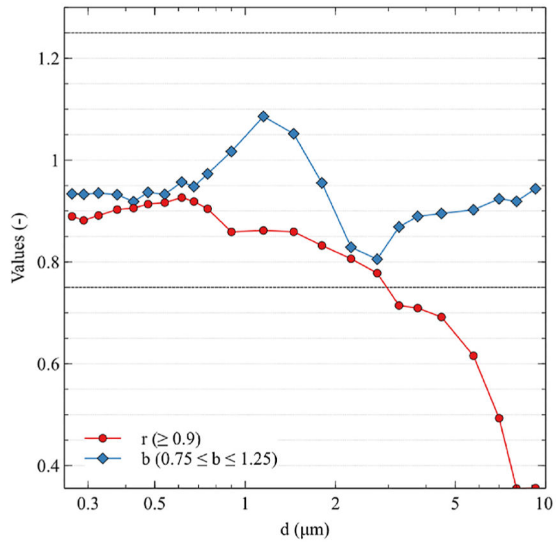

(a)

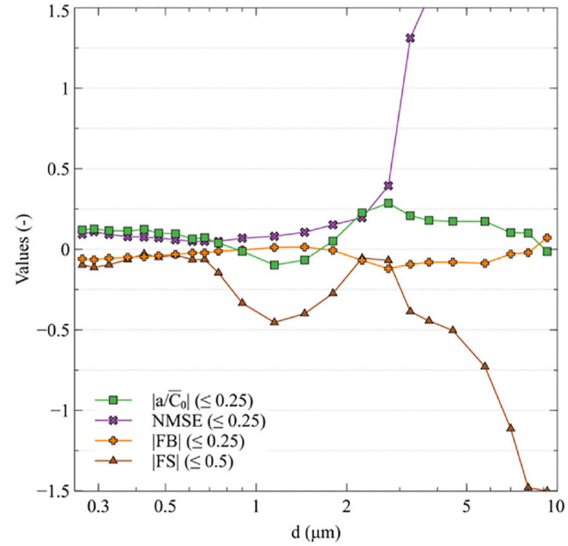

(b)

Fig. 7.

Comparison of model accuracy metrics by particle size. The conditions in parentheses represent the criteria recommended in ASTM D 5157.

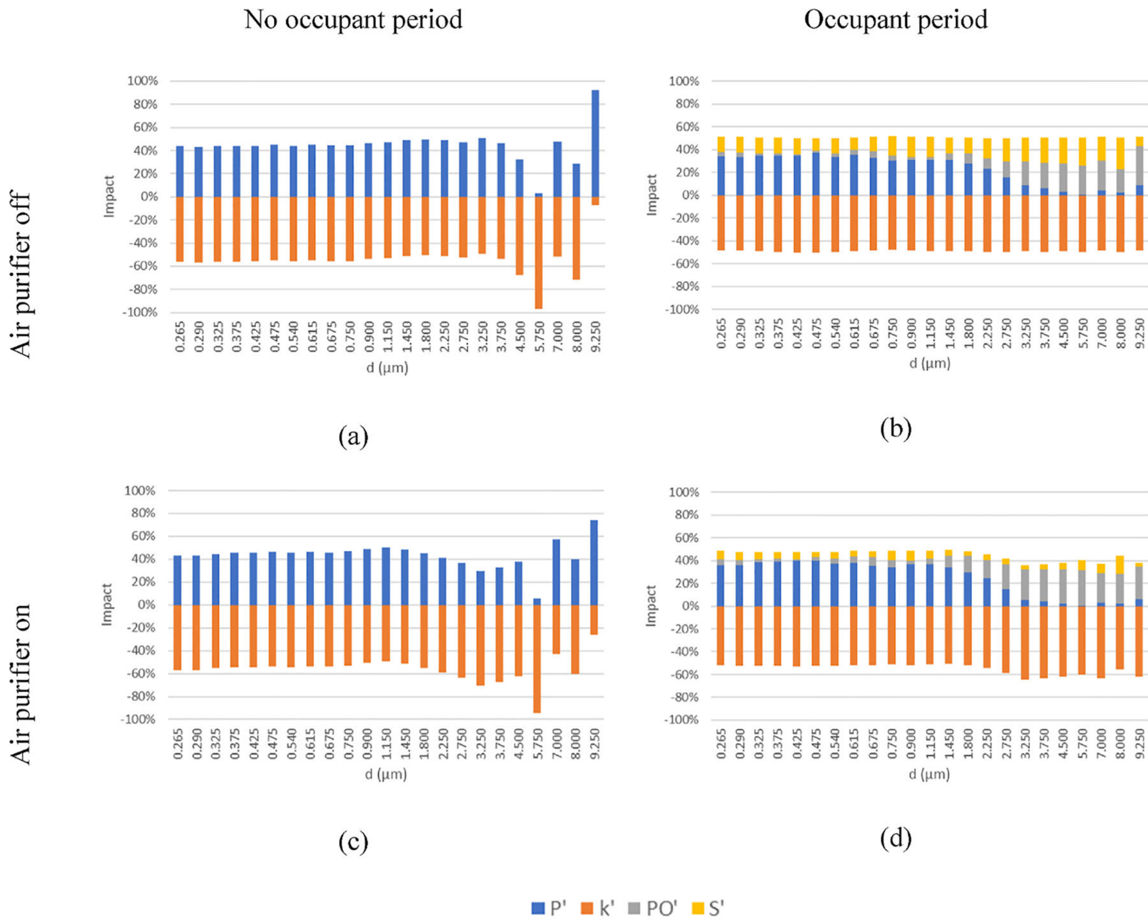

Fig. 8.

Relative contribution of each term (penetration, P'; deposition, k'; door access effect, PO'; and generation/resuspension, $\dot{s}$) in the right-hand side of Eq. (1) to indoor particle concentrations in four scenarios: (a) AP off and no occupant; (b) AP off with occupants; (c) AP on and no occupant; and (d) AP on with occupants.

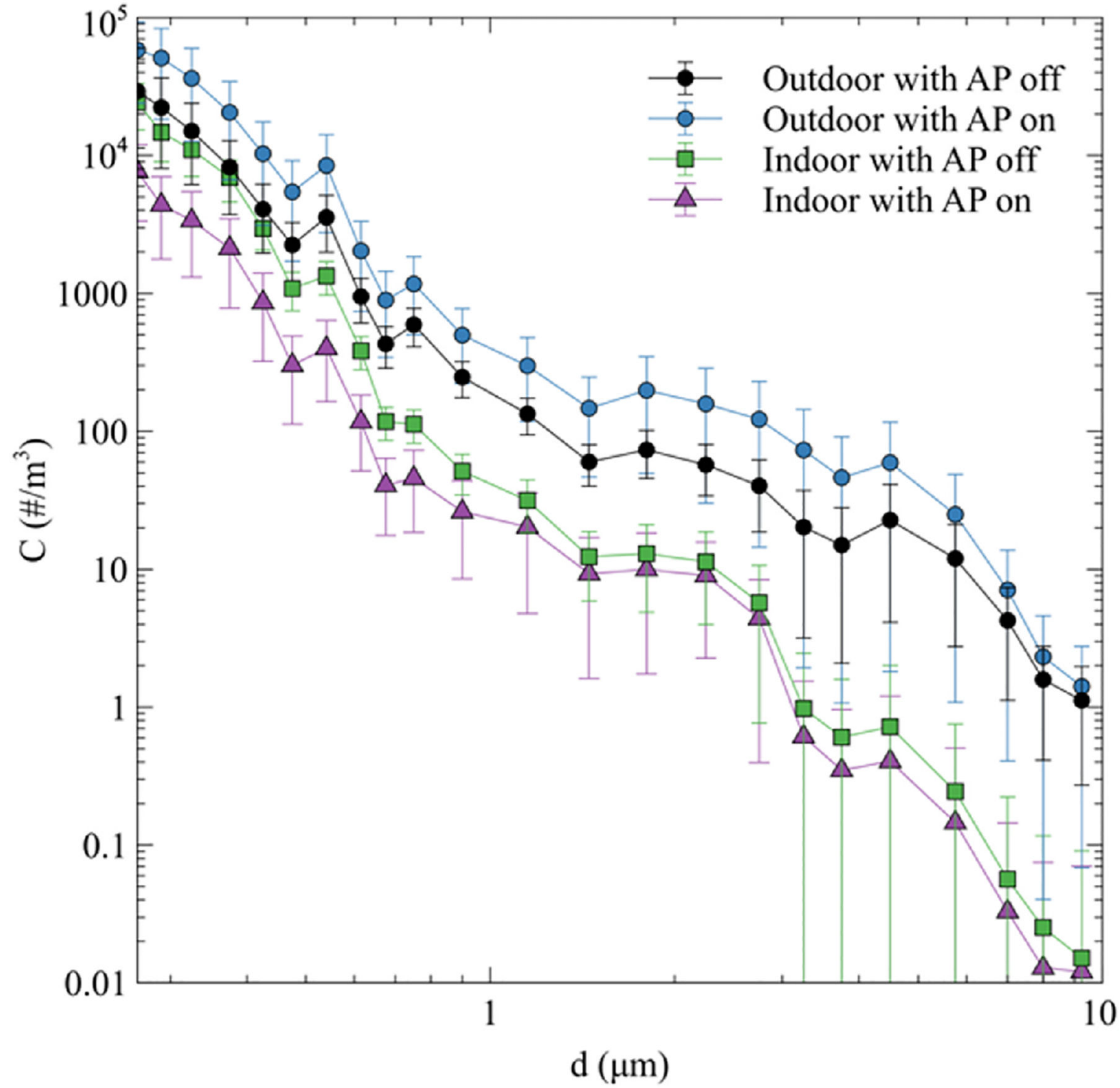

Fig. 9.
Outdoor and indoor particle number concentrations by particle size and AP operation.

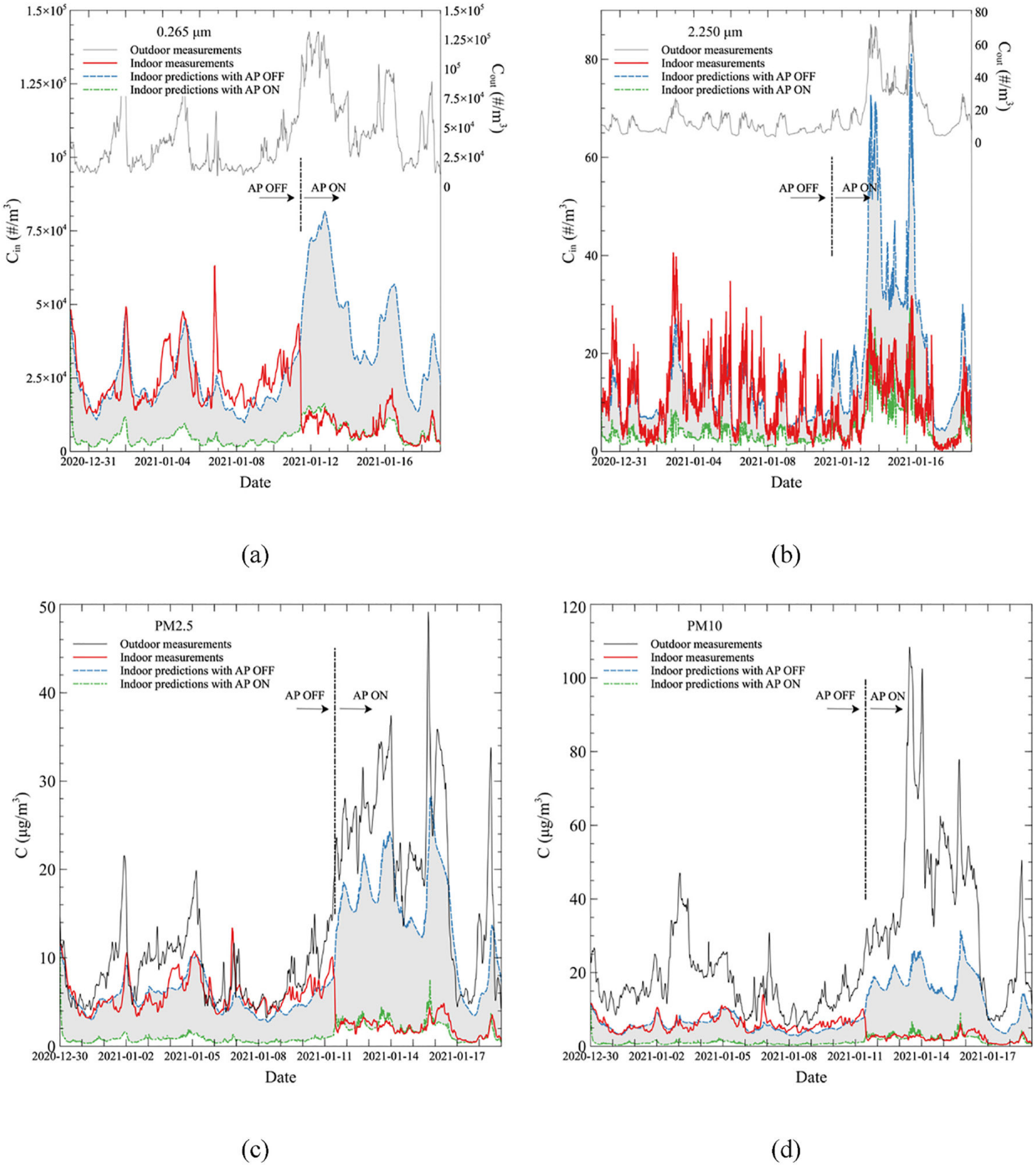

Fig. 10.

Comparison of actual measurements of indoor particle concentrations with the predicted concentrations from the prediction model for (a) 0.265 μm and (b) 2.250 μm channels, (c) $PM_{2.5}$, and (d) PM_{10}. The red real line in the figure represents the measured PM concentrations. The blue dashed line represents the model predictions under no AP operation, and the green dash-dotted line shows the model predictions under AP operation. Before January 11, 2021, the green dash-dotted line is the model predictions for the assumed condition of AP operation while the AP was not operated. After January 11, 2021, the blue dashed line is the model predictions for the assumed condition of no AP operation while the AP was being operated.

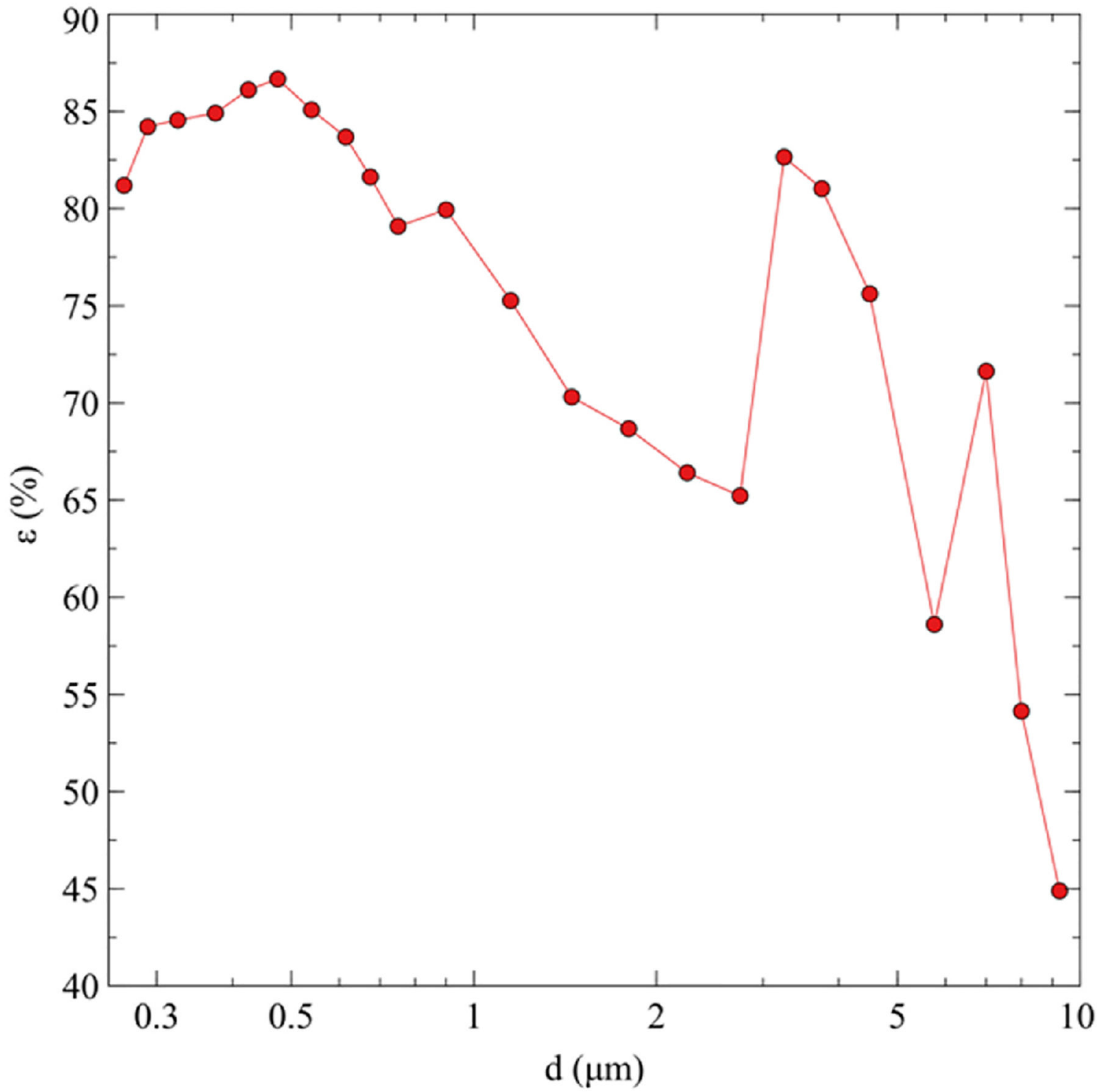

Fig. 11.

Size-specific particle removal effectiveness of AP estimated from the prediction model.

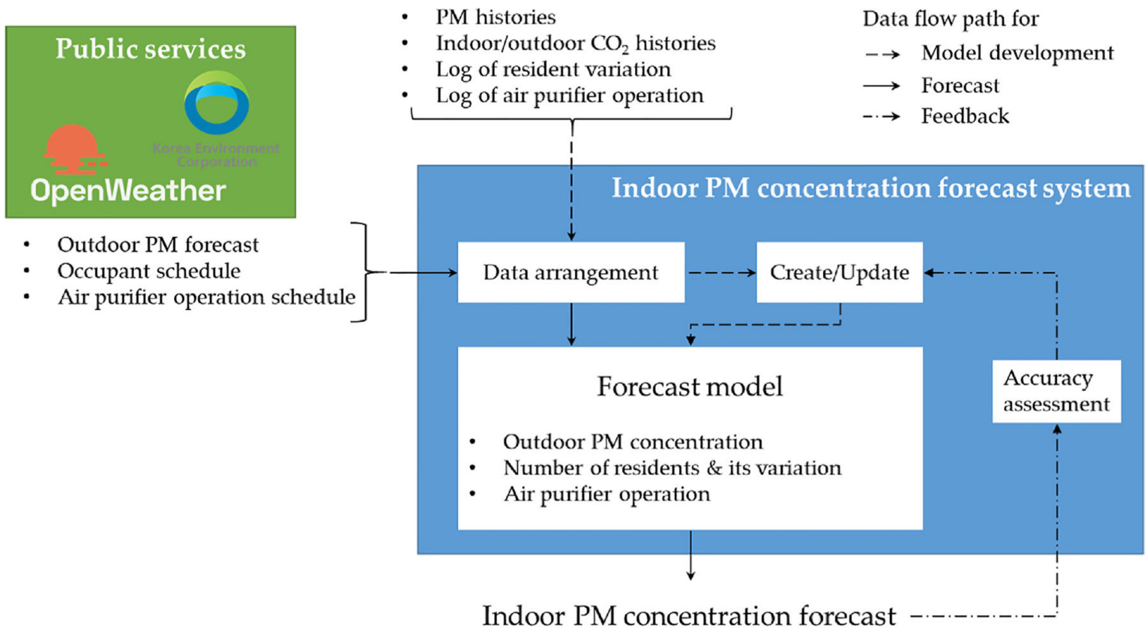

Fig. 12.

Schematic diagram of a forecast system for indoor PM concentrations.

Table 1

Nominal channels for particle diameters of 10 μm or smaller and size ranges for each channel.

Nominal value (μm)	Range (μm)	Nominal value (μm)	Range (μm)
0.265	0.250–0.280	1.450	1.300–1.600
0.290	0.280–0.300	1.800	1.600–2.000
0.325	0.300–0.350	2.250	2.000–2.500
0.375	0.350–0.400	2.750	2.500–3.000
0.425	0.400–0.450	3.250	3.000–3.500
0.475	0.450–0.500	3.750	3.500–4.000
0.540	0.500–0.580	4.500	4.000–5.000
0.615	0.580–0.650	5.750	5.000–6.500
0.675	0.650–0.700	7.000	6.500–7.500
0.750	0.700–0.800	8.000	7.500–8.500
0.900	0.800–1.000	9.250	8.500–10.000
1.150	1.000–1.300	–	–

Table 2

Parameters determined from the model fitting process for $PM_{2.5}$ and $PM_{2.5-10}$ using Eq. (1).

Term	Unit	$PM_{2.5}$	$PM_{2.5-10}$
P'	$\left(\frac{1}{hour}\right)$	8.536×10^{-2}	$7.054 \times 10^{-3} \pm 1.715 \times 10^{-3}$
k'_{APOFF}	$\left(\frac{1}{hour}\right)$	1.482×10^{-1}	$1.412 \pm 1.510 \times 10^{-1}$
k'_{APON}	$\left(\frac{1}{hour}\right)$	$1.096 \pm 1.573 \times 10^{-2}$	$5.210 \pm 2.087 \times 10^{-1}$
PO'	$\left(\frac{1}{hour \cdot door\ access}\right)$	9.252×10^{-2}	$1.031 \times 10^{-1} \pm 1.069 \times 10^{-2}$
$\dot{s}$	$\left(\frac{\mu g}{m^3 \cdot hour \cdot person}\right)$	1.684×10^{-15}	$1.237 \times 10^{-1} \pm 1.963 \times 10^{-2}$

Author Manuscript

Author Manuscript

Author Manuscript

Table 3

Model performance metrics indicating model fit accuracy for $PM_{2.5}$ and PM_{10}.

	r	b	$a/\bar{C}_o$	NMSE	FB	FS
$PM_{2.5}$	0.905	0.922	0.120	0.069	−0.0470	−0.0451
PM_{10}	0.904	0.914	0.128	0.067	−0.0468	−0.0257

Table 4

Model performance metrics indicating model prediction accuracy for $PM_{2.5}$ and PM_{10}.

	r	b	$a/\bar{C}_o$	**NMSE**	FB	FS
$PM_{2.5}$	0.883	0.876	0.157	0.085	−0.0387	−0.0178
PM_{10}	0.882	0.869	0.164	0.083	−0.0387	−0.0339